Histol Histopathol (2023) 38: 99-112

http://www.hh.um.es

Histology and Histopathology
From Cell Biology to Tissue Engineering

ORIGINAL ARTICLE **Open Access**

Knockdown of circ_0004585 enhances the chemosensitivity of colorectal cancer cells to 5-fluorouracil via the miR-874-3p/CCND1 axis

Shijie Wang[1], Juan Cao[1] and Lijuan Pei[2]

[1]Department of Emergency, Peking University International Hospital and

[2]Department of General Surgery, The Fourth Medical Center of PLA General Hospital, Beijing City, China

Summary. Background. Colorectal cancer (CRC) is a serious threat to human health and is drug-resistant. Circular RNA _0004585 (circ_0004585) has been shown to be expressed in CRC, but whether it plays a role in CRC with chemoresistance remains unknown. Therefore, this study aimed to investigate the potential role of circ_0004585 in CRC with 5-fluorouracil (5-FU) resistance.

Methods. The expression of related genes was detected by quantitative real-time polymerase chain reaction (qRT-PCR), and the protein expressions of cleaved caspase-3, cleaved caspase-9, and cyclin D1 (CCND1) were detected by western blot. Cell functions were identified using CCK-8, colony formation, flow cytometry, tube formation and transwell assays. The putative relationships between miR-874-3p and circ_0004585 or CCND1 were validated by dual-luciferase reporter assays. Animal experiments were conducted to verify the effect of circ_0004585 on 5-FU resistance *in vivo*.

Results. Circ_0004585 was highly expressed in CRC tissues and cells, particularly in 5-FU-resistant CRC tissues and cells. Circ_0004585 knockdown enhanced 5-FU sensitivity to further inhibit CRC cell viability, colony formation, cell migration and invasion, and accelerate cell apoptosis. MiR-874-3p was the target of circ_0004585, and miR-874-3p depletion partially recovered the malignant behaviors of 5-FU-resistant CRC cells that were blocked by silencing of circ_0004585. In addition, CCND1 was the target of miR-874-3p, and overexpression of CCND1 was able to restore the malignant effects of 5-FU-resistant CRC cells that were repressed by miR-874-3p enrichment. Animal experiments confirmed that circ_0004585 knockdown inhibited the growth of CRC tumors and enhanced 5-FU sensitivity *in vivo*.

Conclusion. Circ_0004585 promotes the development of CRC and increases 5-FU resistance in CRC through the miR-874-3p/CCND1 axis. These results suggest that circ_0004585 may be a therapeutic target for 5-FU-ressitant CRC.

Key words: circ_0004585, miR-874-3p, CCND1, Colorectal cancer, 5-fluorouracil

Introduction

Colorectal cancer (CRC) is the second most fatal cancer in the world, accounting for 13% of all cancers (Lech et al., 2016; Chen et al., 2019a; Wang et al., 2020). Although CRC can be treated by surgery, drugs and chemotherapy, the existence of chemotherapy resistance leads to a poor prognosis in patients with CRC (Wang et al., 2019). A large amount of clinical data show that 5-fluorouracil (5-FU) is the most common drug used in cancer chemotherapy, but CRC is also resistant to it (Xu et al., 2020). Therefore, it is imperative to explore new therapeutic targets for CRC to reduce its drug resistance.

As a competitive endogenous RNA (ceRNA), circRNAs have been actively studied in tumors in recent years (Arnaiz et al., 2019). It is a kind of non-coding RNA with a unique continuous covalent closed-loop structure, without terminal 5'cap and 3'tail (Memczak et al., 2013; Liu et al., 2017). Several studies have investigated the relationship between circRNAs and CRC. For example, He et al. showed silencing circ_0007031 inhibited the progression of CRC and enhanced the sensitivity of 5-FU *in vivo* and *in vitro* (He et al., 2020). Liu et al. showed that circ_0000231 could be used to regulate the occurrence and development of CRC (Liu et al., 2020). Tian et al. found that circ_0004585 may promote cancer metastasis of CRC (Tian et al., 2019). However, the role of circ_0004585 in

Corresponding Author: Lijuan Pei, Department of General Surgery, The Fourth Medical Center of PLA General Hospital, No.51 Fucheng Road, Haidian District, Beijing 100048, China. e-mail: Huilongguan304@163.com

DOI: 10.14670/HH-18-502

CRC sensitivity to 5-FU remains unclear.

It is well known that microRNAs (miRNAs) are sponges of circRNAs and can interact with the 3'untranslated region (3'UTR) of mRNA to play a negative regulatory role (Krol et al., 2010; Macfarlane and Murphy, 2010; Melo and Esteller, 2014). Many studies have shown that miRNA is involved in the occurrence and metastasis of tumors (Gregory and Shiekhattar, 2005; Hansen et al., 2013). Similarly, miR-874-3p has been found to play a role in thyroid cancer (Ding et al., 2021), triple negative breast cancer (Wu et al., 2020) and CRC (Que et al., 2017). However, it is unknown whether miR-874-3p and circ_0004585 are related and whether they play a role in CRC.

Cyclin D1 (CCND1), a regulatory subunit that encodes a holoenzyme, regulates gene transcription (Chen et al., 2019b). Studies have reported that CCND1, as an oncogene, is involved in the occurrence of a variety of cancers, such as lung cancer (Yang et al., 2020), liver cancer (Ding et al., 2020) and CRC (Yan et al., 2020). It has been reported that overexpression of CCND1 in CRC can promote metastasis of CRC cells, which may indicate that CCND1 can be used as a new target for treatment of CRC (Feng et al., 2019). However, the role of CCND1 in chemotherapy resistance in CRC is unknown.

In this study, we found that circ_0004585 is highly expressed in CRC, and the knockdown of circ_0004585 can regulate the malignant behavior and drug resistance of CRC cells. Importantly, we investigate the mechanism of circ_0004585/miR-874-3p/CCND1 axis in drug resistance of CRC. Our findings provides a new target for the treatment of CRC and its drug resistance.

Materials and methods

Patients and cell lines

Tumor specimens and paracancerous normal tissues from 39 patients with CRC in Peking University International Hospital were collected, including 15 cases in the 5-FU-sensitive group and 24 cases in the 5-FU-resistant group. According to RECIST 1.1 criteria, CRC patients were divided into 5-FU-sensitive CRC group and 5-FU-resistant CRC group. The sample was immediately frozen in liquid nitrogen. None of the samples received any preoperative treatment. Each patient provided written informed consent and was supervised and directed by the Peking University International Hospital Ethics Committee.

Human normal colorectal cells (NCM460) and human CRC cell lines (HCT116 and HCT8) were purchased from American type culture specimens (ATCC; Manassas, VA, USA). All of these cells were cultured in Dulbecco's modified eagle medium (DMEM; Thermo Fisher, Waltham, MA, USA) supplemented with 10% fetal bovine serum (FBS) and 1% streptomycin and penicillin (Invitrogen, Carlsbad, CA, USA) at 37°C in 5% CO_2 environment. The 5-FU-resistant cells were built by treating normal HCT116 and HCT8 cells with the multiple concentration of 5-FU. 1 μg/mL 5-FU was used for the maintenance of drug resistance in HCT116/FU and HCT8/FU.

Cell transfection

Short interfering RNA (siRNA) targeting circ_0004585 (si-circ_0004585#1 and si-circ_0004585#2) and its corresponding control group (si-NC), miR-874-3p mimics (miR-874-3p), and its negative control (miR-NC), miR-874-3p inhibitor (anti-miR-874-3p) and its matched (anti-miR-NC), CCND1 overexpression vector (CCND1) and matched control (pcDNA) were synthesized by Ribobio Co., Ltd. (Guangzhou, China), and then transfected into HCT116 and HCT8 cells using Lipofectamine 2000 (Thermo Fisher, Waltham, MA, USA).

Quantitative real-time polymerase chain reaction (qRT-PCR)

Trizol Reagent (Thermo Fisher) was used to separate total RNA. Then the total RNA was then reverse-transcribed using Reverse Transcription Kit (Thermo Fisher). In terms of miRNA reverse transcription, the MicroRNA Reverse Transcription Kit (Thermo Fisher) was utilized to treat total RNA. Afterwards, qRT-PCR was performed for cDNA using SYBR Green qRT-PCR Mix (Takara, Shiga, Japan) according to the manufacturer's protocol. GAPDH or U6 were used as internal reference, and the relative expression was calculated by $2^{-\Delta\Delta CT}$. The forward and reverse primers were displayed as below:

GAPDH, F: 5'-GGAGCGAGATCCCTCCAAAAT-3'
R: 5'-GGCTGTTGTCATACTTCTCATGG-3'
U6, F: 5'-CTCGCTTCGGCAGCACA-3'
R: 5'-AACGCTTCACGAATTTGCGT-3'
circ_0004585, F: 5'-TCACAGAGGACTCCTACCCG-3'
R: 5'-GGGAAGCAGGTCAGAGTGAG-3'
miR-874-3p, F: 5'- GCCGAGCTGCCCTGGCCCGA-3'
R: 5'-CAGTGCGTGTCGTGGAGT-3'
miR-431-5p, F: 5'-GCCGAGTGTCTTGCAGGCCGT-3'
R: 5'-CAGTGCGTGTCGTGGAGT-3'
miR-589-5p, F: 5'- GCCGAGTGAGAACCACGTCT-3'
R: 5'-CAGTGCGTGTCGTGGAGT-3'
miR-339-3p F: 5'-GGGTGAGCGCCTCGGCGACA-3'
R: 5'-CAGTGCGTGTCGTGGAGT-3'
miR-338-3p, F: 5'- TGCGGTCCAGCATCAGTGAT-3'
R: 5'-CAGTGCGTGTCGTGGAG -3'
miR-1278, F: 5'-GCCGAGTAGTACTGTGCATA-3'
R: 5'-CAGTGCGTGTCGTGGAGT-3'
CCND1, F: 5'-TCACTGAGGGAGTACGTGGA-3'
R: 5'-AGCAGTGCAGTCTACTTCGG-3'

Western blot analysis

Total protein was separated from CRC tissues or cells using Radioimmunoprecipitation analysis buffer

(RIPA; Thermo Fisher), and BCA protein assay kit (Pierce; Rockford, IL, USA) was used to quantify the total protein. The protein samples were loaded into 12% SDS-PAGE and the separated protein bands were next transferred to PVDF membranes. After blocking the membranes with 5% skim milk, the primary antibodies, such as anti-β-actin (1:1,000, ab8226, Abcam, Cambridge, MA, USA), anti-cleaved casp3 (cleaved casp3; 1:1000, ab2302, Abcam), anti-cleaved casp9 (1:1000, ab2324, Abcam), and anti-CCND1 (1:5000, ab226977, Abcam), were used to incubate the membranes at 4°C conditions overnight. Subsequently, the membranes were exposed to goat-anti rabbit secondary antibody (1:20000, ab205718, Abcam) at room temperature for 1 h. The protein bands on the membrane were visualized using BeyoECL Plus kit (Beyotime, Shanghai, China).

Cell Counting Kit-8 assay

HCT116, HCT116/FU, HCT8, and HCT8/FU cells were seeded into 96-well plates. Then 5-FU solution at the dose of 0.1, 0.5, 1, 10 and 100 μg/mL (MedChem Express; CAS No. 51-21-8) was used to incubate cells for 24 hours. CCK-8 kit (Thermo Fisher) was added into each well to culture cells for 2 hours. The absorbance at 450 nm was determined using a microplate analyzer (BioTek, Winooski, Vermont, USA).

Colony formation assay

The transfected cells were seeded into 6-well plates (200 cells/well) and incubated 2 weeks, then the colonies were fixed with paraformaldehyde (Beyotime), and dyed with crystal violet (Beyotime). The colonies were observed and counted under a light microscope (Nikon, Tokyo, Japan).

Flow cytometry assay

The transfected cells were eluted with PBS and suspended with 1×binding buffer from the Annexin-FITC and Propidium iodide Apoptosis Detection kit (BD Biosciences, San Diego, CA, USA). In brief, cells suspended in Annexin-FITC binding buffer were stained with Annexin-FITC and propidium iodide (PI) in the dark in accordance with the protocol. Finally, the apoptotic cells were detected by flow cytometry (BD Biosciences).

Transwell assay

Transwell chambers coated with or without Matrigel (Corning, New York, Madison, USA) were used for the ability of CRC cell invasion or migration, respectively. In brief, a total of 5×10^4 cells in serum-free culture medium were added into the upper transwell chambers. Meanwhile, the lower transwell chambers were added with fresh culture medium containing 10% FBS. After 24 hours of culture, the upper cells were wiped with a cotton swab, and the cells at lower surface were fixed with methanol for 20 min and stained with crystalline violet dye (0.1%) for 20 min. Three images were selected at random to count the number of migrated or invaded cells under a high-powered microscope.

Tube formation assay

The 48-well plates were covered with Matrigel (Corning). After Matrigel curing for 1 h, 200 μL cell medium of CRC cells with different treatments was inoculated into the wells to culture human umbilical vein endothelial cells (HUVECs, Procell, Wuhan, China). After incubation for 4-6h, the number of tubes was observed under a microscope and photos were taken. The ImageJ software (NIH, Bethesda, Maryland, USA) was used to quantify the rate of tube formation.

Dual-luciferase reporter assay

The sequences of circ_0004585 or CCND1 3'UTR containing presumed miR-874-3p interacting sites were cloned into pGL3-basic vectors (Realgene, Nanjing, China), respectively. Cells in 48-well plates (8×10^3 cells/well) were co-transfected with luciferase reporter plasmid in combination with miR-874-3p or miR-NC using Lipofectamine 2000. The relative luciferase activities were measured by Dual-Luciferase Reporter Assay Kit (GeneCopoeia, Rockville, MD, USA) after transfection for 48 hours, with Renilla luciferase activity as control.

Xenograft models

All animal experiments were carried out in accordance with the instructions of Peking University International Hospital Animal Care and Use Committee. Experimental mice (BALB/c, female, 6-8 weeks of age) were purchased from Beijing Weidahe Laboratory Animal Science and Technology Co., Ltd. (Beijing, China). The small hairpin RNA (sh-circ_0004585) and shRNA negative control (sh-NC) targeting circ_0004585 were obtained from Ribobio Co., Ltd. (Guangzhou, China). HCT116 cells (2×10^6) with the infection of lentivirus-packaged sh-NC or sh-circ_0004585 were subcutaneously injected into BALB /c mice (n=5). After 7 days, 5-FU (1 μg/mL) or PBS was injected into tumors every 5 days. Tumor volumes were measured every 5 days, and tumor weight was measured after 32 days. Tumor volume was calculated according to the formula: volume =1/2 (length×width^2). The expression of circ_0004585 and miR-874-3p were analyzed by qRT-PCR, and the protein expression of CCND1 was analyzed by western blot.

Statistical analysis

GraphPad Prism 7 (GraphPad, San Diego, CA, USA) was utilized for data analysis. Difference

comparison between groups were determined using Student's t-test. Pearson's correlation analysis was applied to measure the correlation between two groups. Each experiment was carried out at least three times and the final data were shown as the mean ± standard deviation (SD). $P<0.05$ meant significant difference.

Results

Circ_0004585 was highly expressed in 5-FU-resistant CRC

In order to investigate the role of circ_0004585 in CRC, the expression of circ_0004585 in CRC tissues was detected by qRT-PCR, as shown in Fig. 1a. Compared with normal tissues, the expression of circ_0004585 was increased in CRC tissues, and its expression was higher in 5-FU-resistant cancer tissues than that in 5-FU-sensitive cancer tissues. CCK-8 results showed that HCT116/FU and HCT8/FU cells were resistant to 5-FU treatment relative to HCT116 and HCT8 cells (Fig. 1b,c), suggesting that 5-FU-resistant CRC cell lines were successfully established. In addition, circ_0004585 was highly expressed in CRC cells (HCT116 and HCT8) in comparison to non-cancer cells (NCM460) (Fig. 1d), and its expression was higher in HCT116/FU and HCT8/FU cells in comparison to their parental cells (Fig. 1e,f). In general, circ_0004585 is highly expressed in CRC and may be associated with 5-FU resistance.

Knockdown of circ_0004585 reduced cell proliferation and promoted apoptosis in CRC cells

We next identified the biological function of circ_0004585 in CRC cells and 5-FU-resistant CRC cells. The transfection efficiency of si-circ_0004585 is shown in Figure 2a, and the inhibitory effect of si-circ_0004585#1 was higher than that of si-circ_0004585#2, so si-circ_0004585#1-transfected cells were selected in subsequent experiments. CCK-8 test results showed that cell viability was significantly reduced in the 5-FU group and si-circ_0004585#1 alone transfected group, and circ_0004585 knockdown increased 5-FU sensitivity and further reduced cell viability (Fig. 2b,c). Similarly, the clone formation experiment found that the proliferation of HCT116 and HCT8 cells was suppressed by 5-FU treatment or si-circ_0004585#1 transfection, and circ_0004585 silencing might enhance 5-FU effects and further block the colony-forming ability of HCT116 and HCT8 cells (Fig. 2d,e). In addition, we found that si-circ_0004585#1 transfection or 5-FU treatment significantly increased the apoptosis of HCT116 and HCT8 cells, and the co-treatment of si-circ_0004585#1+5-FU further enhanced the apoptosis rate of these cells (Fig. 3a,b). Western blot results showed that cleaved casp3 and cleaved casp9 protein levels were significantly increased in the 5-FU

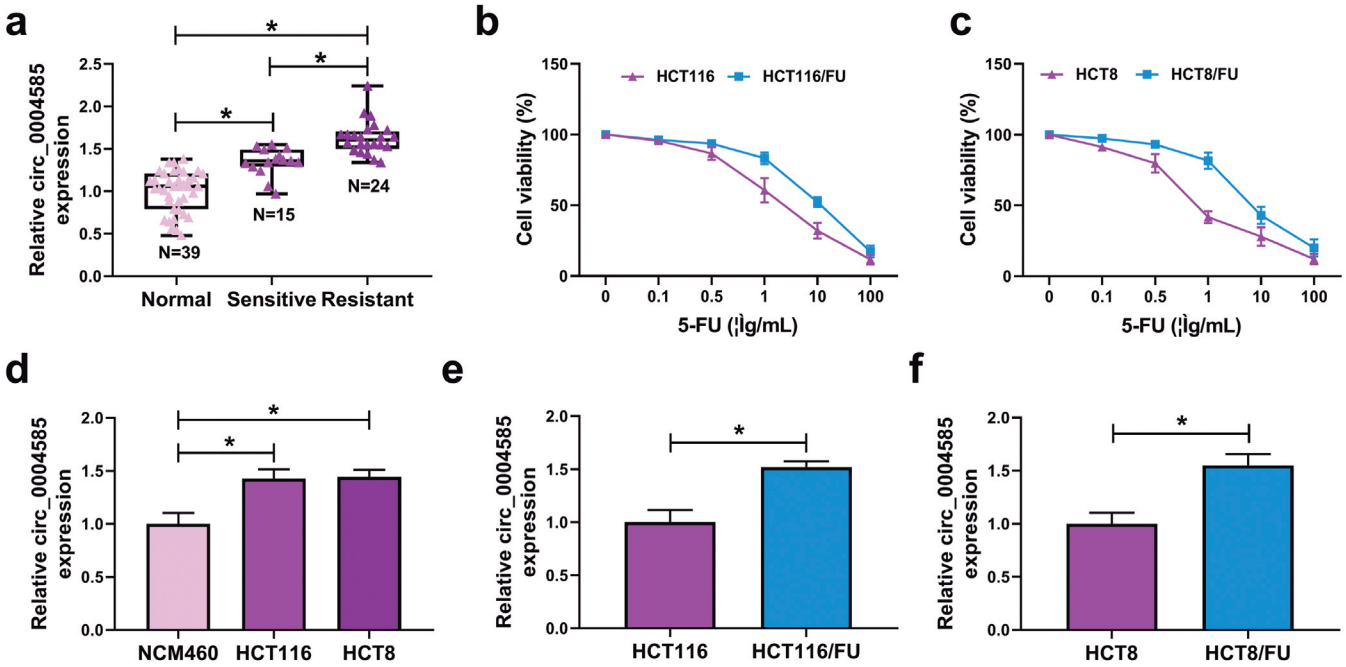

Fig. 1. Circ_0004585 is up-regulated in 5-FU-resistant CRC tissues and cells. **a.** The expression of circ_0004585 in normal tissues (n=39), 5-FU-sensitive tissues (n=15) and 5-FU-resistant tissues (n=24) were detected by qRT-PCR. **b, c.** CCK-8 assay was used to detect cell viability of HCT116/FU, HCT8/FU, HCT116 and HCT8 cells after 5-FU treatment. **d.** The expression of circ_0004585 in HCT116, HCT8 and NCM460 cells was measured by qRT-PCR. **e, f.** Circ_0004585 expression in HCT116/FU, HCT8*FU and their parental cells was checked by qRT-PCR. *$P<0.05$.

group or si-circ_0004585#1 alone transfected group, and their levels were even higher in the si-circ_0004585#1+5-FU group (Fig. 3c). In conclusion, silencing of circ_0004585 increased the sensitivity of CRC cells to 5-FU and thus inhibited the proliferation of HCT116 and HCT8 cells but promoted cell apoptosis.

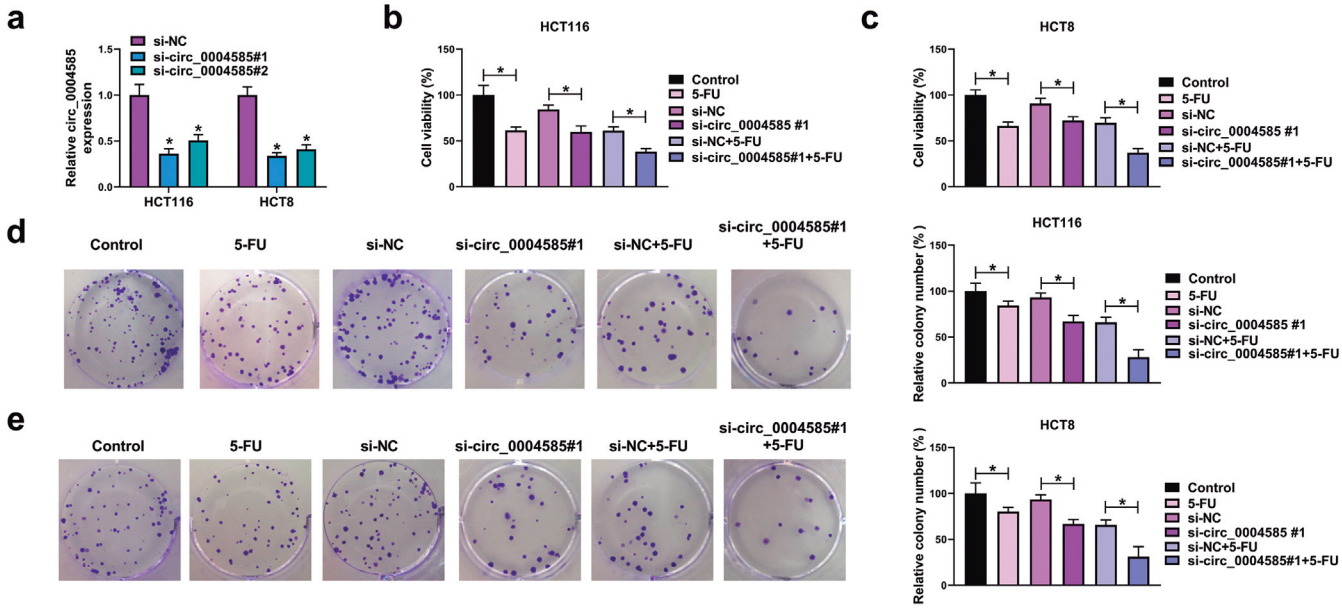

Fig. 2. Silencing circ_0004585 reduced cell viability and colony formation in CRC cells. **a.** The knockdown efficiency of circ_0004585 was detected by qRT-PCR. **b-e.** The experiments were conducted in 6 cell groups, including Control, 5-FU, si-NC, si-circ_0004585#1, si-NC+5-FU and si-circ_0004585#1+5-FU. **b, c.** CCK-8 assay was used to examine the cell viability. **d, e.** Cell proliferation was evaluated by colony formation assay. *P<0.05.

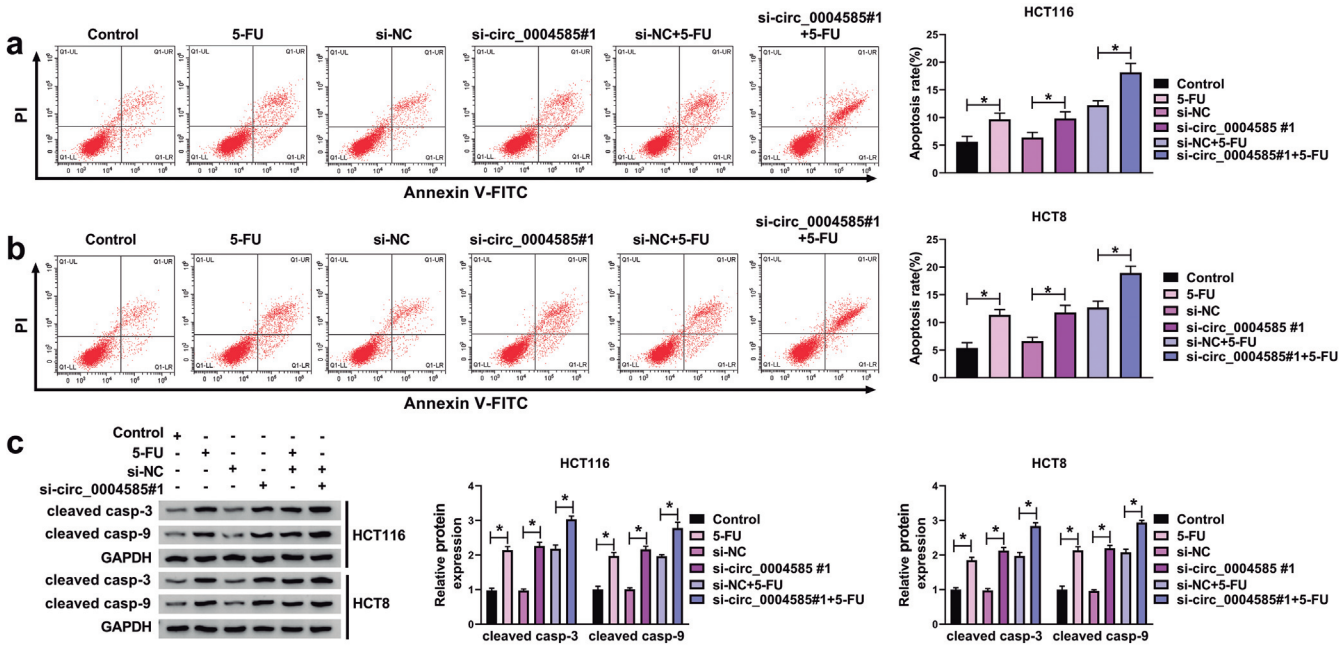

Fig. 3. Silencing circ_0004585 enhanced cell apoptosis in CRC cells. **a-c.** The experiments were conducted in 6 cell groups, including Control, 5-FU, si-NC, si-circ_0004585#1, si-NC+5-FU and si-circ_0004585#1+5-FU. **a, b.** Flow cytometry analysis was utilized to assess cell apoptosis. **c.** Western blot showed the expression of cleaved casp3 and cleaved casp9 proteins. *P<0.05.

Down-regulation of circ_0004585 reduced cell tube formation and metastasis in CRC cells

Functionally, tube formation test results showed that compared with the control group, tube formation was significantly reduced in the 5-FU group or si-circ_0004585#1-transfected group, and tube formation ability further declined in the si-circ_0004585#1+5-FU treatment group (Fig. 4a,b). Compared with the matched control group, the ability of cell migration and invasion was significantly reduced by 5-FU treatment or circ_0004585 silencing, and circ_0004585 silencing was able to enhance 5-FU effects and further diminished the ability of cell migration and invasion (Figs. 4c,d, 5a,b).

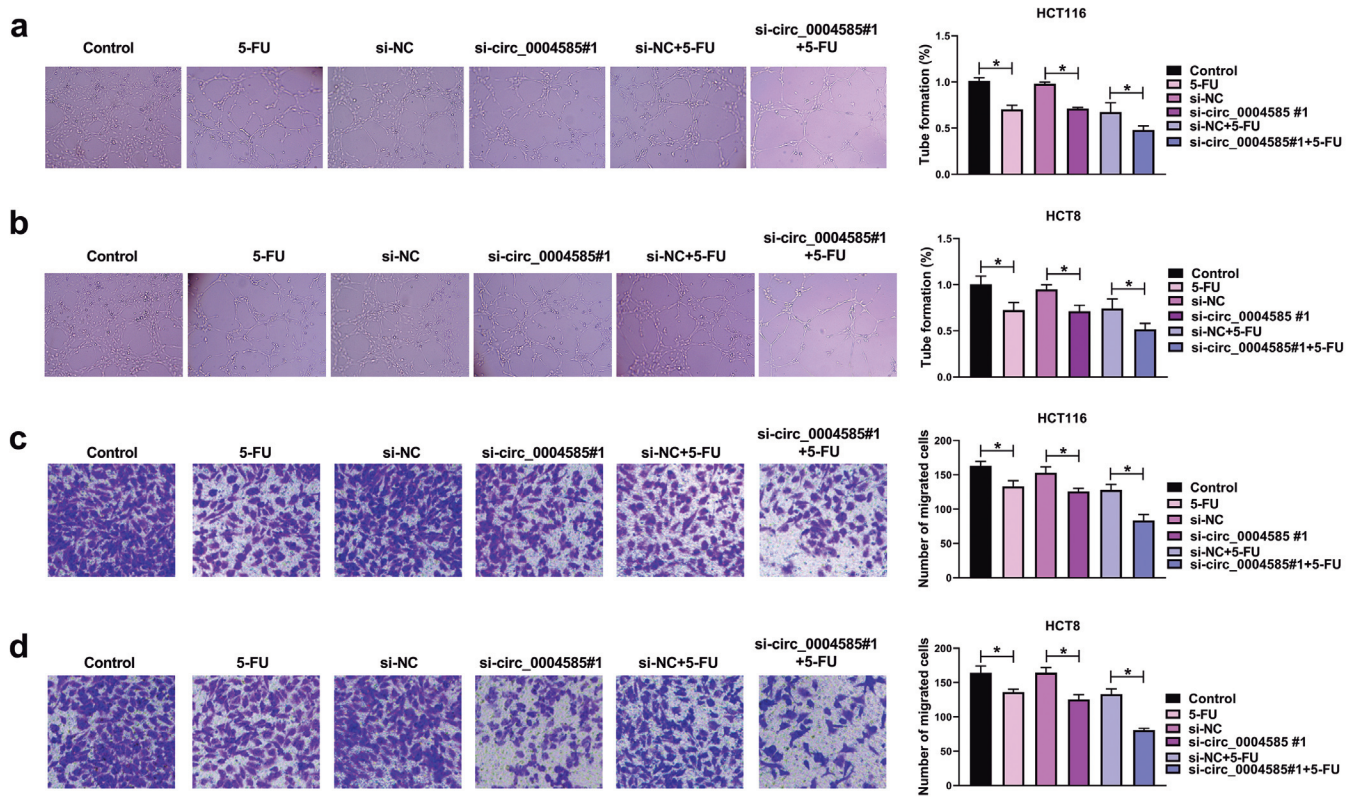

Fig. 4. Knockdown of circ_0004585 reduced cell angiogenesis and migration in CRC cells. **a-d.** The experiments were conducted in 6 cell groups, including Control, 5-FU, si-NC, si-circ_0004585#1, si-NC+5-FU and si-circ_0004585#1+5-FU. **a, b.** Tube formation assay was used to examine the number of branches. **c, d.** Transwell assay was used to assess cell migration. **P*<0.05.

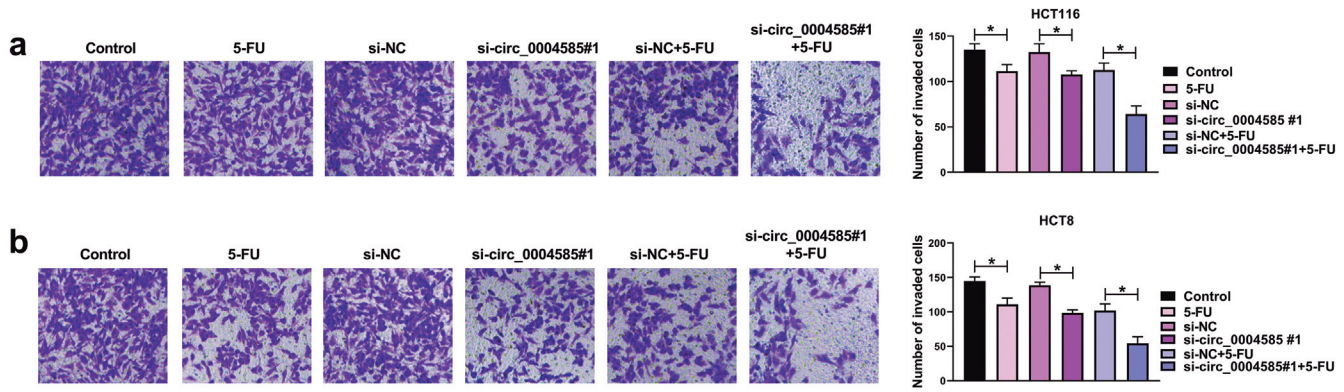

Fig. 5. Knockdown of circ_0004585 reduced cell invasion in CRC cells. **a, b.** Transwell assay was used to assess cell invasion in the following groups, including Control, 5-FU, si-NC, si-circ_0004585#1, si-NC+5-FU and si-circ_0004585#1+5-FU. **P*<0.05.

In short, knockdown of circ_0004585 increased the sensitivity of CRC cells to 5-FU and thus inhibited the tube-formation, migration and invasion of HCT116 and HCT8 cells.

Knockdown of circ_0004585 reduced cell viability, tube formation, migration and invasion but promoted apoptosis in 5-FU-resistant CRC cells

Next, in order to identify the biological function of circ_0004585 in CRC resistant cells, it was transfected into HCT116/FU and HCT8/FU cells. CCK-8 results showed that si-circ_0004585#1 could significantly reduce the resistance to 5-FU in HCT116/FU and HCT8/FU cells (Fig. 6a,b). Si-circ_0004585#1 significantly reduced the activity of HCT116/FU and HCT8/FU cells (Fig. 6c). Similarly, the clone formation assay showed that si-circ_0004585#1 inhibited the proliferation of HCT116/FU and HCT8/FU cells (Fig. 6d). Also, si-circ_0004585#1 promoted the apoptosis of HCT116/FU and HCT8/FU cells (Fig. 6e). Western blot results showed that silencing circ_0004585 promoted cleaved casp3 and cleaved casp9 protein expression (Fig. 6f,g). Next, silencing circ_0004585 inhibited angiogenesis in HCT116/FU and HCT8/FU cells (Fig. 6h). Finally, Transwell experiments showed that knockdown of circ_0004585 could significantly inhibit cell migration and invasion (Fig. 6i,j). In short, silencing circ_0004585 inhibits the malignant behavior in CRC resistant cells.

MiR-874-3p was a target of circ_0004585

As shown in Fig. 7a, we predicted that circ_0004585 had six miRNAs with binding sites using three bioinformatics prediction sites, Starbase (http://starbase.sysu.edu.cn/agoClipRNA.php?source=mRNA), circinteractome (https://circinteractome.nia.nih.gov/mirna_target_sites.html) and circBank (http://www.circbank.cn/). Then, qRT-PCR was used to

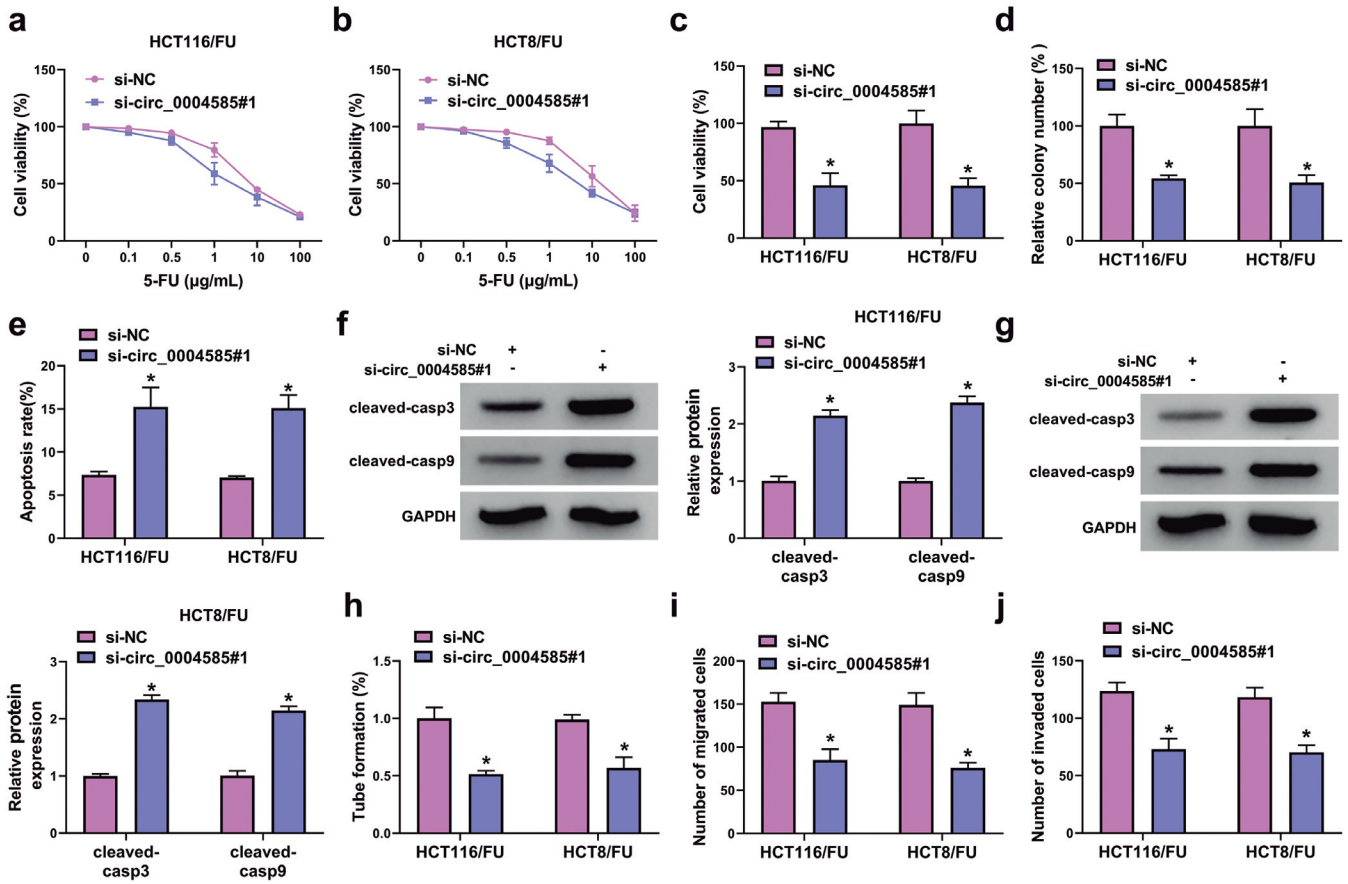

Fig. 6. Knockdown of circ_0004585 promotes the malignant behavior of CRC resistant cells. (a-j) HCT116/FU and HCT8/FU cells were transfected with si-circ_0004585#1 or si-NC. **a, b.** The sensitivity of HCT116/FU and HCT8/FU cells to 5-FU was detected by CCK-8. **c.** Cell viability was detected by CCK-8. **d.** The role of circ_0004585 knockdown on cell proliferation was monitored by colony formation assay. **e.** Flow cytometry was used to detect cell apoptosis. **f, g.** The expression of cleaved casp3 and cleaved casp9 affected by circ_0004585 knockdown was detected by western blot. **h.** Tube formation assay was used to examine the number of branches. **i, j.** Transwell assay was used to assess migration and invasion of HCT116/FU and HCT8/FU cells. **P*<0.05.

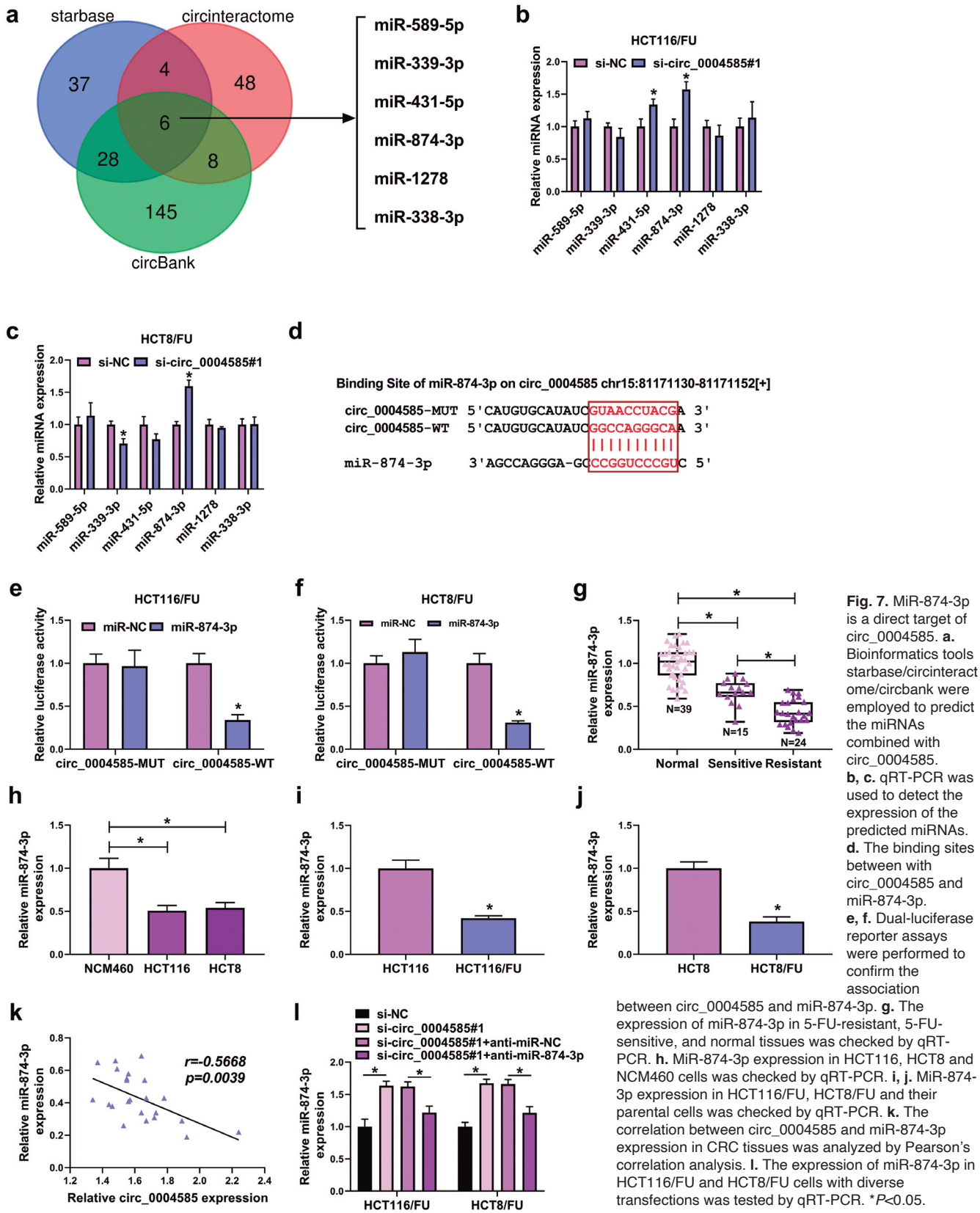

Fig. 7. MiR-874-3p is a direct target of circ_0004585. **a.** Bioinformatics tools starbase/circinteractome/circbank were employed to predict the miRNAs combined with circ_0004585. **b, c.** qRT-PCR was used to detect the expression of the predicted miRNAs. **d.** The binding sites between with circ_0004585 and miR-874-3p. **e, f.** Dual-luciferase reporter assays were performed to confirm the association between circ_0004585 and miR-874-3p. **g.** The expression of miR-874-3p in 5-FU-resistant, 5-FU-sensitive, and normal tissues was checked by qRT-PCR. **h.** MiR-874-3p expression in HCT116, HCT8 and NCM460 cells was checked by qRT-PCR. **i, j.** MiR-874-3p expression in HCT116/FU, HCT8/FU and their parental cells was checked by qRT-PCR. **k.** The correlation between circ_0004585 and miR-874-3p expression in CRC tissues was analyzed by Pearson's correlation analysis. **l.** The expression of miR-874-3p in HCT116/FU and HCT8/FU cells with diverse transfections was tested by qRT-PCR. **P*<0.05.

detect six miRNAs, and it was found that only the expression level of miR-874-3p was significantly up-regulated after circ_0004585 knockdown in HCT116/FU and HCT8/FU cells (Fig. 7b,c). Fig. 7d shows the binding sites of circ_0004585 and miR-874-3p. The results of dual-luciferase report analysis showed that circ_0004585-WT was able to bind to miR-874-3p and reduce the fluorescence activity, while circ_0004585-MUT could not (Fig. 7e,f). The expression of miR-874-3p was significantly decreased in CRC tissues, and was even lower in drug-resistant tissues (Fig. 7g). Similarly, qRT-PCR detection showed that the expression of miR-874-3p was significantly decreased in HCT116 and HCT8 cells and was even lower in HCT116/FU and HCT8/FU cells (Fig. 7h-j). Pearson's correlation analysis showed that miR-874-3p was negatively correlated with circ_0004585 (Fig. 7k). The qRT-PCR results showed that knockdown of circ_0004585 significantly up-regulated the expression of miR-874-3p, and the expression of miR-874-3p was partially retuned after co-transfection with miR-874-3p inhibitor (Fig. 7l). In a word, miR-874-3p is a direct target of circ_0004585.

The effect of si-circ_0004585#1 on cell behaviors was eliminated by miR-874-3p inhibitor in CRC cells

Next, we further explored the relationship between circ_0004585 and miR-874-3p by using a complementary experiment. CCK-8 results showed that anti-miR-874-3p could recover the resistance to 5-FU in HCT116/FU and HCT8/FU cells decreased by si-circ_0004585#1 (Fig. 8a,b). Si-circ_0004585#1 significantly reduced the activity of HCT116/FU and HCT8/FU cells, while anti-miR-874-3p partially recovered it (Fig. 8c). Similarly, the clone formation assay showed that si-circ_0004585#1 inhibited the proliferation of HCT116/FU and HCT8/FU cells, while anti-miR-874-3p partially up-regulated it (Fig. 8d). Also, anti-miR-874-3p inhibited the promoting effect of si-circ_0004585#1 on the apoptosis of HCT116/FU and HCT8/FU cells. (Fig. 8e). Western blot results showed that after addition of miR-874-3p inhibitor, the up-regulated cleaved casp3 and cleaved casp9 protein level was decreased due to the silencing of circ_0004585 (Fig. 8f,g). Next, silencing circ_0004585

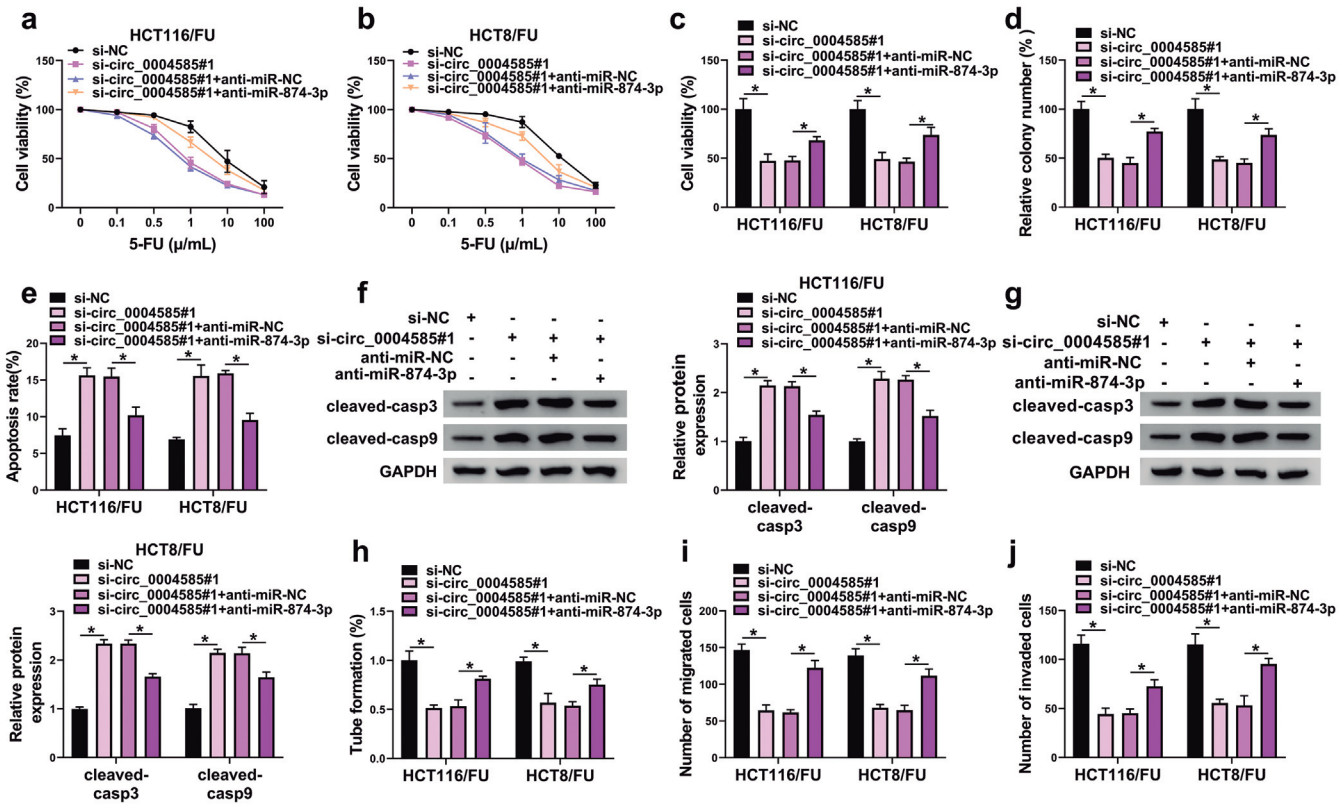

Fig. 8. Anti-miR-874-3p reversed the effect of si-circ_0004585 in CRC resistant cells. HCT116/FU and HCT8/FU cells were transfected with si-NC, si-circ_0004585#1, si-circ_0004585#1+anti-miR-NC or si-circ_0004585#1+anti-miR-874-3p. **a, b.** The sensitivity of transfected HCT116/FU and HCT8/FU cells to 5-FU was detected by CCK-8. **c.** Cell viability was detected by CCK-8. **d.** Cell proliferation was monitored by colony formation assay. **e.** Flow cytometry was used to detect cell apoptosis. **f, g.** The expression of cleaved casp3 and cleaved casp9 was detected by western blot. **h.** Tube formation assay was used to examine the number of branches. **i, j.** Transwell assay was used to assess migration and invasion of transfected HCT116/FU and HCT8/FU cells. **P*<0.05.

inhibited the tube formation in HCT116/FU and HCT8/FU cells, while anti-miR-874-3p partially up-regulated it (Fig. 8h). Finally, Transwell experiments showed that knockdown of circ_0004585 could significantly inhibit cell migration and invasion, while -miR-874-3p inhibitor partially up-regulated it (Fig. 8i,j). In short, anti-miR-874-3p can recover the effect of si-circ_0004585#1 in HCT116/FU and HCT8/FU cells.

CCND1 was a target of miR-874-3p

As shown in Figure 9a, Starbase predicted the binding sites of miR-874-3p and CCND1. The results of dual-luciferase report analysis showed that CCND1 3'UTR-WT could bind to miR-874-3p and reduce the fluorescence activity, while CCND1 3'UTR-MUT could not (Fig. 9b,c). Mechanically, qRT-PCR results showed that CCND1 expression was increased in CRC compared

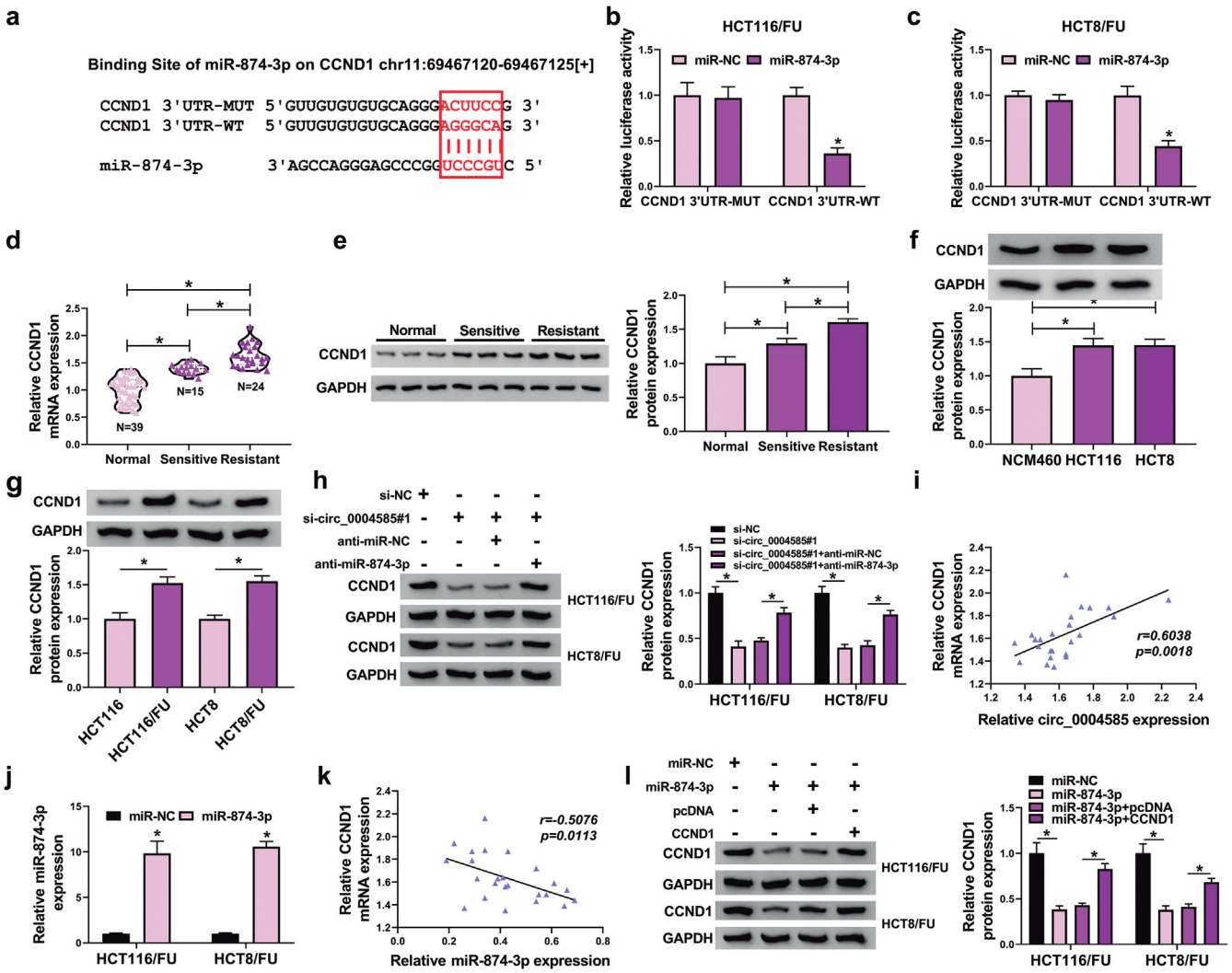

Fig. 9. CCND1 is a direct target of miR-874-3p. **a.** Bioinformatics tool starbase was utilized to predict the binding sites between miR-874-3p and CCND1 3'UTR. **b, c.** Dual-luciferase reporter assays were performed to confirm the association between CCND1 and miR-874-3p. **d.** QRT-PCR showed the expression of CCND1 in 5-FU-resistant, 5-FU-sensitive, and normal tissues. **e.** The protein level of CCND1 in 5-FU-resistant, 5-FU-sensitive, and normal tissues was measured by western blot. **f.** The protein level of CCND1 in HCT116, HCT8 and NCM460 cells was measured by western blot. **g.** The protein level of CCND1 in HCT116/FU, HCT8/FU and their parental cells was checked by western blot. **h.** The expression of CCND1 protein in HCT116/FU and HCT8/FU cells transfected with si-NC, si-circ_0004585#1, si-circ_0004585#1+anti-miR-NC or si-circ_0004585#1+anti-miR-874-3p was tested by western blot assay. **i.** The correlation between circ_0004585 and miR-874-3p expression was analyzed by Pearson's correlation analysis. **j.** The expression of miR-874-3p in HCT116/FU and HCT8/FU cells with miR-NC or miR-874-3p transfection was tested by qRT-PCR. **k.** The correlation between CCND1 and miR-874-3p expression was analyzed by Pearson's correlation analysis. **l.** The expression of CCND1 protein in HCT116/FU and HCT8/FU cells after miR-NC, miR-874-3p, miR-874-3p+pcDNA or miR-874-3p+CCND1 transfection was tested by western blot. **P*<0.05.

with normal tissues, and was more significantly increased in 5-FU resistant tissues (Fig. 9d). Moreover, western blot analysis showed that CCND1 protein was significantly increased in CRC tissues and cells, and the expression was higher in drug-resistant tissues and cells (Fig. 9e-g). Functionally, the miR-874-3p inhibitor could significantly recover the reduced CCND1 protein due to knockdown of circ_0004585 detected by western blot (Fig. 9h). Also, Pearson's correlation analysis showed that CCND1 was positively correlated with circ_0004585 (Fig. 9i). QRT-PCR tested the transfection efficiency of miR-874-3p overexpression in HCT116/FU and HCT8/FU cells (Fig. 9j). Pearson's correlation analysis showed that miR-874-3p was negatively correlated with CCND1 (Fig. 9k). Finally, western blot analysis showed that overexpression of miR-874-3p down-regulated the expression of CCND1, while co-transfection of overexpression of CCND1 partially restored the expression level of CCND1 (Fig. 9l). In conclusion, CCND1 is a direct target gene of miR-874-3p.

Overexpression of CCND1 relieved the inhibitory action of miR-874-3p up-regulation on cell viability, migration, and invasion in CRC cells.

Next, we further explored the relationship between CCND1 and miR-874-3p by using a complementary experiment. CCK-8 results showed that overexpression of CCND1 could callback the resistance to 5-FU in HCT116/FU and HCT8/FU cells decreased by miR-874-3p (Fig. 10a,b). MiR-874-3p significantly reduced the activity of HCT116/FU and HCT8/FU cells, while overexpression of CCND1 partially up-regulated it (Fig. 10c). Similarly, the clone formation assay showed that miR-874-3p inhibited the proliferation of HCT116/FU and HCT8/FU cells, while overexpression of CCND1 partially up-regulated it (Fig. 10d). Moreover, CCND1 inhibited the promoting effect of miR-874-3p

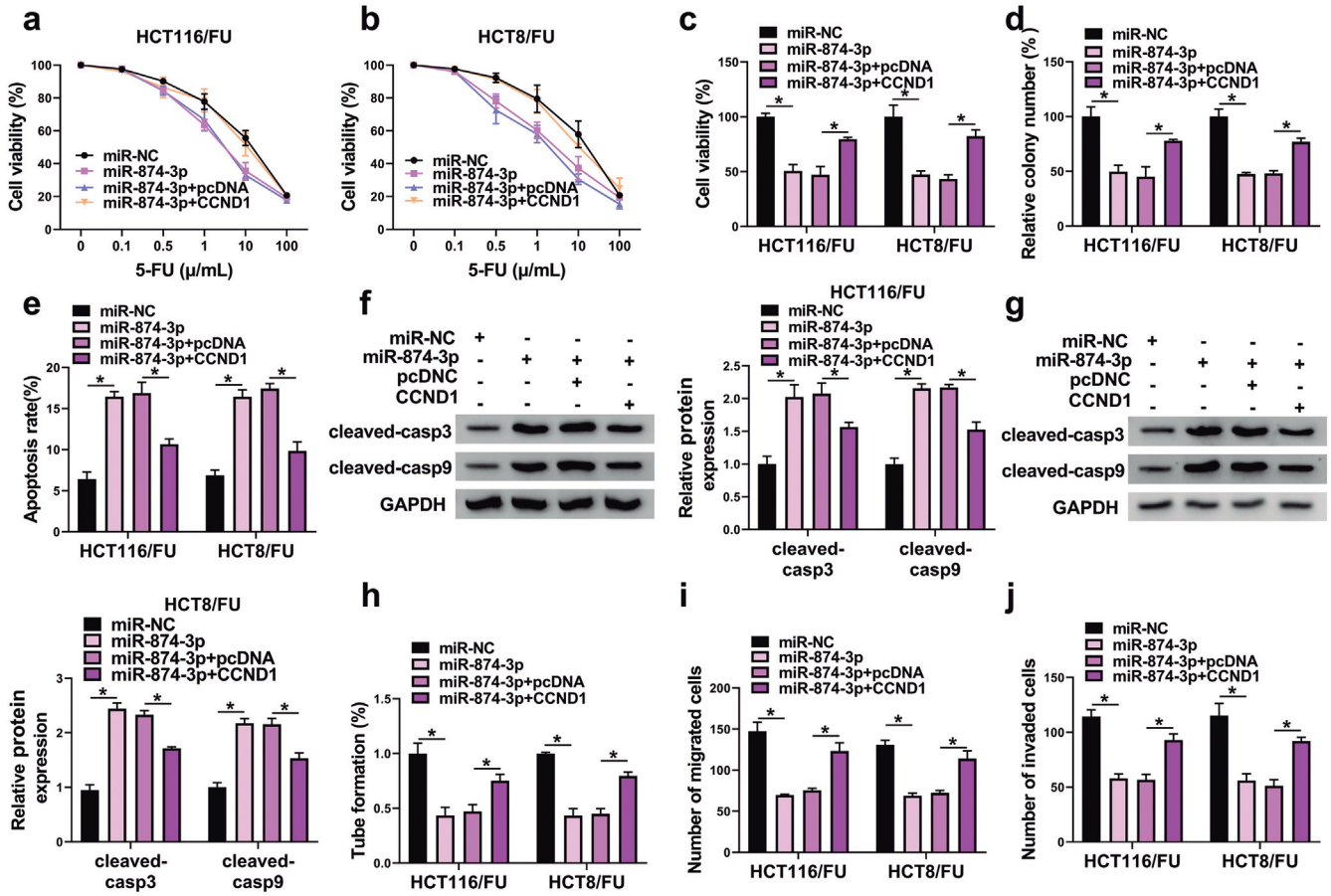

Fig. 10. Overexpression of CCND1 reversed the effect of overexpression of miR-874-3p in CRC resistant cells. HCT116/FU and HCT8/FU cells after miR-NC, miR-874-3p, miR-874-3p+pcDNA or miR-874-3p+CCND1 transfection were used in the following assays. **a, b.** The sensitivity of transfected HCT116/FU and HCT8/FU cells to 5-FU was detected by CCK-8. **c.** Cell viability was detected by CCK-8. **d.** Cell proliferation was monitored by colony formation assay. **e.** Flow cytometry was used to detect cell apoptosis. **f, g.** The expression of cleaved casp3 and cleaved casp9 was detected by western blot. **h.** Tube formation assay was used to examine the number of branches. **i, j.** Transwell assay was used to assess migration and invasion of transfected HCT116/FU and HCT8/FU cells. *P<0.05.

overexpression on the apoptosis of HCT116/FU and HCT8/FU cells. (Fig. 10e). Western blot results showed that co-transfection overexpression of CCND1 decreased cleaved casp3 and cleaved casp9 protein levels up-regulated by miR-874-3p (Fig. 10f,g). Next, miR-874-3p overexpression inhibited tube formation in HCT116/FU and HCT8/FU cells, while CCND1 partially up-regulated it (Fig. 10h). Finally, Transwell experiments showed that miR-874-3p could significantly inhibit cell migration and invasion, while overexpression of CCND1 partially up-regulated it (Fig. 10i,j). In short, overexpression of CCND1 can recover the effect of overexpression of miR-874-3p in HCT116/FU and HCT8/FU cells.

Circ_0004585 knockdown inhibited tumor growth in vivo and enhanced 5-FU effects

In order to better explore the influence of circ_0004585 on drug resistance in CRC, we constructed a CRC xenotransplantation model. By recording and observing tumor volume (Fig. 11a) and tumor weight (Fig. 11b), we found that intratumoral injection of sh-circ_0004585 combined with 5-FU could significantly inhibit tumor growth. Then, qRT-PCR was used to analyze the expression of circ_0004585 and miR-874-3p, and the results showed that circ_0004585 expression was reduced in the sh-circ_0004585-administered group and further reduced in the sh-circ_0004585+5-Fu-administered group. However, miR-874-3p expression was reinforced in the sh-circ_0004585-administered group and further reinforced in the sh-circ_0004585+5-Fu-administered group (Fig. 11c). Finally, western blot results showed that knockdown of circ_0004585 or 5-FU treatment could significantly reduce the protein level of CCND1, while co-treatment of sh-circ_0004585 and 5-FU had the greatest degree of down-regulation of CCND1 expression (Fig. 11d). In conclusion, down-regulation of circ_0004585 can reduce drug resistance in CRC.

Discussion

Numerous studies have demonstrated that the crosstalk of ceRNA via shared miRNAs is involved in the pathogenesis of human diseases including cancer (Karreth and Pandolfi, 2013). More and more reports have shown that circRNAs, as endogenous non-coding RNA, play an indispensable role in numerous cancers, such as esophageal cancer (Li et al., 2020), ovarian

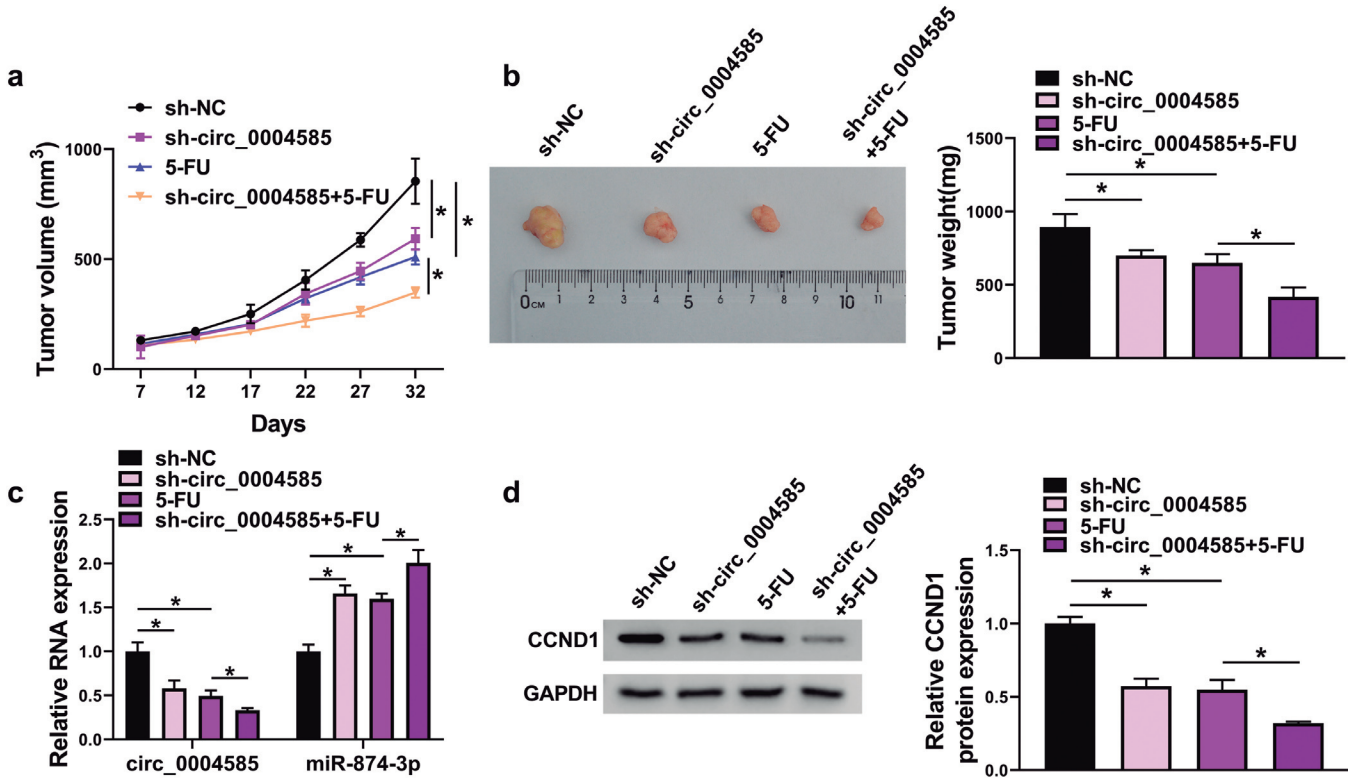

Fig. 11. Circ_0004585 knockdown inhibited tumor growth *in vivo*. Xenograft models in nude mice were administered with sh-NC, sh-circ_0004585, 5-FU or sh-circ_0004585+5-FU. **a, b.** Tumor volume and weight in different groups were measured to assess tumor growth. **c.** Relative expression levels of circ_0004585 and miR-874-3p in xenograft models were detected by qRT-PCR. **d.** CCND1 protein level was tested by western blot in xenograft models. **P*<0.05.

cancer (Hou and Zhang, 2020), and CRC (Jin et al., 2019). Here we show, for the first time, circ_0004585 acts as a novel regulator of CRC cell functional characteristics and drug resistance by regulating the miR-974-3p/CCND1 axis.

The mechanism of circRNAs in cancer progression has become a new research hotspot. For example, in CRC, circ_001680 is highly expressed in CRC tissues, and silencing circ_001680 blocks the proliferation and metastasis of CRC cells (Jian et al., 2020). In addition, a recent finding showed that circ_0004585 is upregulated in tissues and cells of patients with CRC and also has a poor prognosis (Tian et al., 2019), but it has not been reported in the study of chemotherapy in CRC. Consistent with these findings, in this study, we verified that the expression of circ_0004585 was abnormally enhanced in CRC tissues and cell lines. Functionally, silencing circ_0004585 inhibited CRC cell viability, proliferation, migration, and invasion *in vitro*. In addition, the downregulation of circ_0004585 also inhibited tumor growth in nude mice and increased tumor sensitivity to 5-FU, suggesting that circ_0004585 may play a carcinogenic role in CRC and may increase the drug resistance of CRC.

According to the report, circRNAs can function as a sponge miRNA. Starbase, circinteractome and circBank all predicted that circ_0004585 had binding sites with miR-874-3p, and it was reported that miR-874-3p was significantly down-regulated in CRC cells, and the overexpression of miR-874-3p enhanced the chemical sensitivity to 5-FU (Que et al., 2017; Zhang et al., 2020). This conclusion is consistent with our research. First, we verified that the expression of miR-874-3p was significantly reduced in CRC tissues and cells. Subsequently, the correlation between miR-874-3p and circ_0004585 was verified by a complementary experiment, and the results showed that there was a negative regulatory effect between the two. Furthermore, functional analysis showed that miR-874-3p inhibitors restored inhibition of CRC cell proliferation, migration, and invasion due to circ_0004585 knockdown. It was confirmed that circ_0004585 can regulate the development of CRC cells by targeting miR-874-3p.

MiRNA inhibits the target gene through the 3'UTR sequence of the complementary mRNA. In this study, targeted binding of miR-874-3p to CCND1 was predicted by starbase. Many recent studies have shown that CCND1 can promote the development of CRC, which is consistent with our findings (Guo and Xue, 2020; Yan et al., 2020). Our study showed that CCND1 was elevated in CRC tissues and cells. Functionally, CCND1 eliminated the inhibitory effect of miR-874-3p overexpression on CRC cell proliferation. Mechanically, CCND1 protein expression was detected by co-transfection of si-circ_0004585#1 and miR-874-3p. The mechanism of action of circ_0004585/miR-874-3p/CCND1 in CRC cells was further supported.

In summary, we found that circ_0004585 positively regulates CCND1 through sponging miR-874-3p, thereby promoting CRC progression and 5-FU resistance. These findings provide new targets for follow-up research and treatment of CRC.

Acknowledgements. None

Disclosure of interest. The authors declare that they have no conflicts of interest

Funding. None.

Ethics approval and consent to participate. Written informed consent was obtained from patients with approval by the Institutional Review Board in Peking University International Hospital.

Consent for publication. Not applicable.

Availability of data and materials. Please contact the correspondence author for the data request.

Authors' contribution. Shijie Wang was responsible for drafting the manuscript. Shijie Wang and Juan Cao contributed to the analysis and interpretation of data. Shijie Wang and Lijuan Pei contributed in the data collection. All authors read and approved the final manuscript.

References

Arnaiz E., Sole C., Manterola L., Iparraguirre L., Otaegui D. and Lawrie C.H. (2019). CircRNAs and cancer: Biomarkers and master regulators. Semin. Cancer Biol. 58, 90-99.

Chen H., Li N., Ren J., Feng X., Lyu Z., Wei L., Li X., Guo L., Zheng Z., Zou S., Zhang Y., Li J., Zhang K., Chen W., Dai M., He J. and group of Cancer Screening Program in Urban C. (2019a). Participation and yield of a population-based colorectal cancer screening programme in China. Gut 68, 1450-1457.

Chen I.X., Chauhan V.P., Posada J., Ng M.R., Wu M.W., Adstamongkonkul P., Huang P., Lindeman N., Langer R. and Jain R.K. (2019b). Blocking CXCR4 alleviates desmoplasia, increases T-lymphocyte infiltration, and improves immunotherapy in metastatic breast cancer. Proc. Natl. Acad. Sci. USA 116, 4558-4566.

Ding H., Wang Y. and Zhang H. (2020). CCND1 silencing suppresses liver cancer stem cell differentiation and overcomes 5-fluorouracil resistance in hepatocellular carcinoma. J. Pharmacol. Sci. 143, 219-225.

Ding Y., Wu L., Zhuang X., Cai J., Tong H., Si Y., Zhang H., Wang X. and Shen M. (2021). The direct miR-874-3p-target FAM84A promotes tumor development in papillary thyroid cancer. Mol. Oncol. 15, 1597-1614.

Feng Y., Qian W., Zhang Y., Peng W., Li J., Gu Q., Ji D., Zhang Z., Wang Q., Zhang D. and Sun Y. (2019). CDCA2 promotes the proliferation of colorectal cancer cells by activating the AKT/CCDN1 pathway *in vitro* and *in vivo*. BMC Cancer 19, 576.

Gregory R.I. and Shiekhattar R. (2005). MicroRNA biogenesis and cancer. Cancer Res. 65, 3509-3512.

Guo F. and Xue J. (2020). MicroRNA6285p inhibits cell proliferation and induces apoptosis in colorectal cancer through downregulating ccnd1 expression levels. Mol. Med. Rep. 21, 1481-1490.

Hansen T.B., Kjems J. and Damgaard C.K. (2013). Circular RNA and miR-7 in cancer. Cancer Res. 73, 5609-5612.

He X., Ma J., Zhang M., Cui J. and Yang H. (2020). Circ_0007031 enhances tumor progression and promotes 5-fluorouracil resistance in colorectal cancer through regulating miR-133b/ABCC5 axis. Cancer Biomark 29, 531-542.

Hou W. and Zhang Y. (2020). Circ_0025033 promotes the progression of ovarian cancer by activating the expression of LSM4 via targeting

miR-184. Pathol. Res. Pract. 217, 153275.

Jian X., He H., Zhu J., Zhang Q., Zheng Z., Liang X., Chen L., Yang M., Peng K., Zhang Z., Liu T., Ye Y., Jiao H., Wang S., Zhou W., Ding Y. and Li T. (2020). Hsa_circ_001680 affects the proliferation and migration of CRC and mediates its chemoresistance by regulating bmi1 through miR-340. Mol. Cancer 19, 20.

Jin C., Wang A., Liu L., Wang G. and Li G. (2019). Hsa_circ_0136666 promotes the proliferation and invasion of colorectal cancer through miR-136/SH2B1 axis. J. Cell Physiol. 234, 7247-7256.

Karreth F.A. and Pandolfi P.P. (2013). CeRNA cross-talk in cancer: When ce-bling rivalries go awry. Cancer Discov. 3, 1113-1121.

Krol J., Loedige I. and Filipowicz W. (2010). The widespread regulation of microRNA biogenesis, function and decay. Nat. Rev. Genet. 11, 597-610.

Lech G., Slotwinski R., Slodkowski M. and Krasnodebski I.W. (2016). Colorectal cancer tumour markers and biomarkers: Recent therapeutic advances. World J. Gastroenterol. 22, 1745-1755.

Li X., Song L., Wang B., Tao C., Shi L. and Xu M. (2020). Circ0120816 acts as an oncogene of esophageal squamous cell carcinoma by inhibiting miR-1305 and releasing TXNRD1. Cancer Cell Int. 20, 526.

Liu J., Liu T., Wang X. and He A. (2017). Circles reshaping the RNA world: From waste to treasure. Mol. Cancer 16, 58.

Liu Y., Li H., Ye X., Ji A., Fu X., Wu H. and Zeng X. (2020). Hsa_circ_0000231 knockdown inhibits the glycolysis and progression of colorectal cancer cells by regulating miR-502-5p/MYO6 axis. World J. Surg. Oncol. 18, 255.

Macfarlane L.A. and Murphy P.R. (2010). MicroRNA: Biogenesis, function and role in cancer. Curr. Genomics 11, 537-561.

Melo S.A. and Esteller M. (2014). Disruption of microRNA nuclear transport in human cancer. Semin. Cancer Biol. 27, 46-51.

Memczak S., Jens M., Elefsinioti A., Torti F., Krueger J., Rybak A., Maier L., Mackowiak S.D., Gregersen L.H., Munschauer M., Loewer A., Ziebold U., Landthaler M., Kocks C., le Noble F. and Rajewsky N. (2013). Circular RNAs are a large class of animal RNAs with regulatory potency. Nature 495, 333-338.

Que K., Tong Y., Que G., Li L., Lin H., Huang S., Wang R. and Tang L. (2017). Downregulation of miR-874-3p promotes chemotherapeutic resistance in colorectal cancer via inactivation of the hippo signaling pathway. Oncol. Rep. 38, 3376-3386.

Tian J., Xi X., Wang J., Yu J., Huang Q., Ma R., Zhang X., Li H. and Wang L. (2019). CircRNA hsa_circ_0004585 as a potential biomarker for colorectal cancer. Cancer Manag. Res. 11, 5413-5423.

Wang W., Kandimalla R., Huang H., Zhu L., Li Y., Gao F., Goel A. and Wang X. (2019). Molecular subtyping of colorectal cancer: Recent progress, new challenges and emerging opportunities. Semin. Cancer Biol. 55, 37-52.

Wang Q., Zhao H., Wang Q., Cao H., Aujla G.S. and Zhu H. (2020). Enabling secure wireless multimedia resource pricing using consortium blockchains. Future Generation Computer Systems 110, 696-707.

Wu G., Zhou H., Li D., Zhi Y., Liu Y., Li J. and Wang F. (2020). LncRNA DANCR upregulation induced by TUFT1 promotes malignant progression in triple negative breast cancer via miR-874-3p-SOX2 axis. Exp. Cell Res. 396, 112331.

Xu F., Ye M.L., Zhang Y.P., Li W.J., Li M.T., Wang H.Z., Qiu X., Xu Y., Yin J.W., Hu Q., Wei W.H., Chang Y., Liu L. and Zhao Q. (2020). MicroRNA-375-3p enhances chemosensitivity to 5-fluorouracil by targeting thymidylate synthase in colorectal cancer. Cancer Sci. 111, 1528-1541.

Yan F., Ma Y., Liu L., Li L., Deng J. and Sun J. (2020). Long noncoding RNA HOXD-AS1 promotes the proliferation, migration, and invasion of colorectal cancer via the miR-526b-3p/CCND1 axis. J. Surg. Res. 255, 525-535.

Yang Y., Lu T., Li Z. and Lu S. (2020). FGFR1 regulates proliferation and metastasis by targeting CCND1 in FGFR1 amplified lung cancer. Cell Adh. Migr. 14, 82-95.

Zhang N., Zhang P.P., Huang J.J., Wang Z.Y., Zhang Z.H., Yuan J.Z., Ma E.M., Liu X. and Bai J. (2020). Reduced serum exosomal miR-874 expression predicts poor prognosis in colorectal cancer. Eur. Rev. Med. Pharmacol. Sci. 24, 664-672.

Accepted July 28, 2022